

UNCLASSIFIED

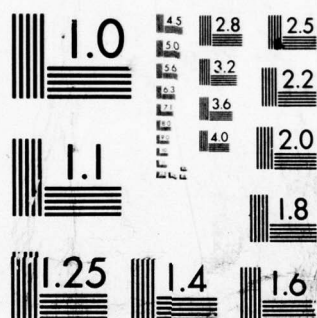
Ball	100
Box	50
Club for me	100
Handicap	100

N00014-75-C-0496
NL

F/G 9/5

END
DATE
FILMED
3-78
DDC

3-78



MICROCOPY RESOLUTION TEST CHART
NATIONAL BUREAU OF STANDARDS-1963-A

AD A 049544

AD No.

JDC FILE COPY

SECURITY CLASSIFICATION OF THIS PAGE (When Data Entered)

REPORT DOCUMENTATION PAGE		READ INSTRUCTIONS BEFORE COMPLETING FORM
1. REPORT NUMBER	2. GOVT ACCESSION NO.	3. RECIPIENT'S CATALOG NUMBER
4. TITLE (and Subtitle)		5. TYPE OF REPORT & PERIOD COVERED
(6) PERFORMANCE LIMITS OF A JOSEPHSON JUNCTION MIXER.		Technical Report 1/31/78 1 Feb 77-31 Jan 78.
7. AUTHOR(s)		6. PERFORMING ORG. REPORT NUMBER
(10) John H. Claassen Naval Research Laboratory, Washington, D.C. 20375 Paul L. Richards		8. CONTRACT OR GRANT NUMBER(s) (15) N00014-75-C-0496 ✓
9. PERFORMING ORGANIZATION NAME AND ADDRESS Department of Physics ✓ University of California Berkeley, California 94720		10. PROGRAM ELEMENT, PROJECT, TASK AREA & WORK UNIT NUMBERS NR 319-055
11. CONTROLLING OFFICE NAME AND ADDRESS Office of Naval Research Physics Program Office Arlington, Virginia 22217		12. REPORT DATE (17) September 1977
14. MONITORING AGENCY NAME & ADDRESS (if different from Controlling Office)		13. NUMBER OF PAGES 53 (12) 56 p.
- id -		15. SECURITY CLASS. (of this report) Unclassified
16. DISTRIBUTION STATEMENT (of this Report) Unlimited		15a. DECLASSIFICATION/DOWNGRADING SCHEDULE
<div style="border: 1px solid black; padding: 5px; text-align: center;"> DISTRIBUTION STATEMENT A Approved for public release; Distribution Unlimited </div>		
17. DISTRIBUTION STATEMENT (of the abstract entered in Block 20, if different from Report)		
18. SUPPLEMENTARY NOTES		
19. KEY WORDS (Continue on reverse side if necessary and identify by block number) Superconductivity - Josephson Effect - Microwave Mixer - Microwave Detector - Infrared Detector		
20. ABSTRACT (Continue on reverse side if necessary and identify by block number) We present the results of extensive analog computer simulations of a Josephson junction used as a mixer with an external local oscillator. The Resistively Shunted Junction model was used throughout, and the effects of intrinsic junction noise were included. When the source impedance is much greater than the junction resistance R our simulations permit predictions of conversion efficiency, noise temperature, and saturation level to be made for a wide range of experimental parameters. The possibility of		

D D C
RECEIVED
FEB 3 1978
RECEIVED

DD FORM 1473

EDITION OF 1 NOV 65 IS OBSOLETE
S/N 0102-LF-014-6601

SECURITY CLASSIFICATION OF THIS PAGE (When Data Entered)

071 970 JOB

20. ABSTRACT (cont'd)

harmonic mixing has also been considered. With a source resistance comparable to R (i.e., conventional "matching") the behavior of the system is too complicated to permit such general predictions of performance. From the results of simulations for a particular set of parameters it appears that the best noise temperature will usually be achieved for a source impedance somewhat greater than R . An upper limit for the mixer noise temperature is $\sim 40 T$ over a broad range of junction parameters, where T is the effective temperature of the junction. The Conversion efficiency under these circumstances should be comparable to what is potentially available from Schottky diode mixers. Our simulations show that with stronger microwave coupling it is possible to obtain conversion gain - i.e., a conversion efficiency exceeding unity. This, however, will probably be at the expense of a higher mixer noise temperature. Saturation can be important even for source temperature ~ 300 K. To avoid saturation it is necessary either to restrict the coupling bandwidth or use an array of junctions.

APPROXIMATELY

ACCESSION FOR	
NTIS	White Section <input checked="" type="checkbox"/>
DDC	Buff Section <input type="checkbox"/>
UNANNOUNCED	<input type="checkbox"/>
JUSTIFICATION	
BY	
DISTRIBUTION/AVAILABILITY CODES	
DIST.	AVAIL. OR/OF SPECIAL
A	

Unlimited Distribution

PERFORMANCE LIMITS OF A JOSEPHSON JUNCTION MIXER

J. H. Claassen and P. L. Richards

September 1977

DDC
RECEIVED
FEB 3 1978
D

"Reproduction in whole or in part is permitted for any purpose of the United States Government."

DISTRIBUTION STATEMENT A

Approved for public release;
Distribution Unlimited

PERFORMANCE LIMITS OF A JOSEPHSON JUNCTION MIXER^{*}

J. H. Claassen[†] and P. L. Richards

Department of Physics, University of California
Berkeley, California 94720

ABSTRACT

We present the results of extensive analog computer simulations of a Josephson junction used as a mixer with an external local oscillator. The Resistively Shunted Junction model was used throughout, and the effects of intrinsic junction noise were included. When the source impedance is much greater than the junction resistance R our simulations permit predictions of conversion efficiency, noise temperature, and saturation level to be made for a wide range of experimental parameters. The possibility of harmonic mixing has also been considered. With a source resistance comparable to R (i.e., conventional "matching") the behavior of the system is too complicated to permit such general predictions of performance. From the results of simulations for a particular set of parameters it appears that the best noise temperature will usually be achieved for a source impedance somewhat greater than R . An upper limit for the mixer noise temperature is $\sim 40 T$ over a broad range of junction parameters, where T is the effective temperature of the junction. The Conversion efficiency under these circumstances should be comparable to what is potentially available from Schottky diode mixers. Our simulations show that with stronger microwave coupling it is possible to obtain conversion gain - i.e., a conversion efficiency exceeding unity. This,

however, will probably be at the expense of a higher mixer noise temperature. Saturation can be important even for source temperatures ~ 300 K. To avoid saturation it is necessary either to restrict the coupling bandwidth or use an array of junctions.

I. INTRODUCTION

An externally supplied rf current has a strong effect on the static current-voltage (I-V) characteristic of a Josephson junction. This dependence is sufficient to make the Josephson junction a candidate as a mixer element for use with an external local oscillator (LO). The sum of a small signal current and a relatively larger LO current is equivalent to an amplitude modulated LO current if the signal is small enough that the phase modulation can be neglected. When the junction is biased in such a way that changes in its I-V curve are observed, a response will be measured at the modulation frequency, which appears at the frequency difference (IF) between the signal and the LO. If the signal is sufficiently small, the output amplitude should be proportional to signal amplitude. This type of mixing in a Josephson junction was first observed by Grimes and Shapiro¹ in 1968.

Because of their high response speed and low operating temperature, Josephson junction mixers show particular promise in the mm wave region as front ends for low noise receivers. The most often quoted figure of merit for a receiver is its single sideband system noise temperature:

$$T_{\text{sys}} = L(T_m + T_{\text{IF}}/\eta). \quad (1)$$

L is the loss between the system input and the mixer, which can in principle be made close to unity, T_{IF} is the noise temperature of the IF (difference frequency) amplifier following the mixer, and T_m is the noise contribution of the mixer referred to the mixer input. The conversion

efficiency η is defined as the ratio of power delivered to the IF amplifier, to the incident signal power. Evidently T_m is the smallest possible system noise temperature that can be achieved by reducing the input losses and the noise of the IF amplifier, and as such represents a limit on performance set by the mixer. Other mixer parameters that can be important are the saturation level and the instantaneous bandwidth. The latter is defined as the range of frequencies around the LO that can be down-converted.

In this paper we will develop predictions of the important figures of merit for Josephson junction mixers, and determine the junction parameters, bias conditions, coupling circuits, etc., that optimize their performance. The mathematical model of a junction (the Resistively Shunted Junction or RSJ model) that was used in our calculations is presented in section II and important scaling parameters are identified. Section III summarizes computer simulations of junction I-V curves under conditions of weak rf coupling. In section IV an expression for conversion efficiency is obtained, both for fundamental and harmonic mixing. It is found that η can exceed unity under some circumstances, and for ideal junctions should have useful values well into the submillimeter region. We then discuss in section V the noise model that is appropriate, and give the results of computer simulations for output noise and the resulting mixer noise temperature of weakly coupled junctions. A simple expression, $T_m \lesssim 40 T$, is found to apply for a broad range of parameters. Saturation effects are estimated in section VI. We find that such effects limit the bandwidth of Josephson junction mixers which are coupled to room temperature sources. The analysis given in this paper builds upon

concepts developed in previous publications of the authors along with their co-worker Y. Taur.^{2,3,4} An attempt has been made, however, to make this discussion self-contained.

When an rf source is strongly coupled to a junction, the computer predictions of η and T_m depend in a complicated way on junction parameters. In section VII we summarize the trends of these dependences for specific choices of parameters. It becomes clear that relatively slight improvements are achieved by strong rf coupling, and then only if rather stringent requirements on junction parameters can be met. In section VIII we explore the possible use of arrays of junctions as mixers. Finally, we conclude in section IX with a discussion of the properties of real junctions that are currently available and that can be expected to become available. The effects on our predictions of self-heating and deviations from the RSJ model are estimated.

II. ELECTRICAL MODEL

The Resistively Shunted Junction (RSJ) model of a Josephson junction that we have used in our calculations, is shown in Fig. 1(a). The Josephson tunneling current path is represented as being in parallel with a linear resistance R , and a capacitance C . The pair tunneling current is given by the well known expression,⁵

$$I_p = I_c \sin \left[\frac{2e}{\hbar} \int^t v(t') dt' \right], \quad (2)$$

where V is the instantaneous voltage across the junction. A theoretical expression connects R with the critical current I_c for at least two kinds of Josephson junctions,^{6,7}

$$RI_c = \pi \Delta^2 / 4ekT_c . \quad (3)$$

Here Δ is the energy gap of the superconductor from which the junction is made, and T_c is its transition temperature. The data from available junctions of many types suggest that (3) gives an approximate universal upper limit for the product of R and I_c that can be obtained. On the other hand, the shunt capacitance C can vary considerably, from negligibly small in microbridges⁸ to quite large in sandwich-type tunnel junctions.⁹

In the theoretical analysis of the RSJ model it is helpful to use the following reduced variables:

$$\text{Current: } i = I/I_c$$

$$\text{Voltage: } v = V/RI_c$$

$$\text{Frequency: } \Omega = h\nu/2eRI_c$$

$$\text{Time: } \tau = t(2eRI_c)/h$$

$$\text{Capacitance: } \beta_c = (2e/h)R^2I_cC$$

$$\text{Impedance: } z = Z/R$$

$$\text{Noise: } \Gamma = 2ekT/\hbar I_c$$

In the last expression, T is the physical junction temperature only if the noise currents in the junction arise primarily from classical Johnson noise in the shunt resistor. If other sources of noise are important it must be considered to be an effective noise temperature.

Practical constraints on the impedance scale are imposed by external coupling considerations. The characteristic impedance levels at both the rf and IF frequencies must in practice be of the order of ten to a few hundred ohms. For most experimental conditions, the junction resistance R is considerably less than the magnitude of any external impedances connected to the junction, so that it is appropriate to consider all externally applied signals as current sources. The case of strongly coupled junctions will be discussed in section VII. If i_x represents the sum of these externally applied currents, the equations which represent the RSJ model of Fig. 1(a) are:

$$v = \frac{d\phi}{d\tau}, \quad (4)$$

$$i_x + i_n = \sin \phi + v + \beta_c \frac{dv}{d\tau}. \quad (5)$$

Here ϕ is the difference between the phases of the superconducting order parameter on either side of the junction. The noise current i_n is usually assumed to have a "white" spectral density, with $\overline{i_n^2} = \frac{2}{\pi} \Gamma \Delta\Omega$. Here $\Delta\Omega$ is the bandwidth over which the noise is observed. However, for very low temperatures a different noise spectrum should be assumed, as will be discussed in a later section.

A considerable fraction of the body of literature on Josephson junctions consists of solutions to Eqs. (4) and (5) under various conditions. A comprehensive summary of the results of these calculations is given in Ref. 10. It should be noted that only for certain special cases are analytic solutions possible. The analog computer has been a powerful

tool in analyzing the Josephson equations since reasonably accurate solutions can be rapidly generated as various parameters are altered. The theoretical results in this paper were all obtained from one or another of the junction simulator schemes that have been published.^{11,12}

III. RESULTS OF MODEL CALCULATIONS

For $\beta_c \geq 0.8$ the static I-V curve with no rf current applied becomes hysteretic in the region near zero voltage³ when $\Gamma = 0$. The current spread of the hysteresis loop increases monotonically with β_c . In the presence of significant rf current, a wide variety of effects occur, including the possibility of hysteretic I-V curves. Hysteretic junctions have not generally been used as mixers,³ since the appropriate bias point (to be discussed in more detail in a subsequent section) is not readily accessible. Sandwich-type tunnel junctions have not been used as mixing elements since these junctions have historically had very large values of β_c , and are strongly hysteretic. The large capacitance also gives a small rf impedance which leads to coupling difficulties.

We shall consider the case of a junction with $\beta_c = 0$ which is driven by dc and rf current sources as a first approximation to the conditions under which a Josephson junction is actually used as a mixer. In reduced units we write $i_x = i_{dc} + i_{rf} \sin \Omega\tau$. Figs. 2(a) and (b) show representative I-V curves with $\Omega < 1$ for various values of rf current. Evidently when $\Gamma = 0$ we can characterize these curves by the dependence of the various step heights on rf current. Unlike the case

$\Omega > 1$, no analytical expressions for the step heights exist when $\Omega < 1$, except in a perturbation theory approximation.¹⁴ Various authors^{15,16,17} have published computer calculations of the step heights for values of $\Omega < 1$.

In this paper we limit our attention to the range $0.1 < \Omega < 1.0$. For normalized frequencies greater than one there is a rapid decline in mixer performance ($\eta \sim \Omega^{-2}$, $T_m \sim \Omega^2$).¹⁰ On the other hand we shall find that performance is not especially improved as Ω is reduced below 0.1. The normalized frequency range we consider can correspond to quite high real frequencies. For Nb junctions whose RI_c product approaches the theoretical limit (3), for example, $\Omega = 1$ corresponds to $\nu \approx 1000$ GHz.

From the point of view of mixing, the dependence of the 0th step i_0 on rf current is of particular interest. We note from Fig. 2(d) that there is a considerable range over which the dc current depends linearly on the rf current. An ac current proportional to di_0/di_{rf} appears in the output when the LO current is amplitude modulated at Ω_{IF} . Fig. 2(d) shows that a LO bias current which reduces the 0th step by 50-80% will produce the maximum IF output current.

In order to consider the case of harmonic mixing (where the detected signal is near $N\Omega_{LO}$, with N an integer), we have generalized the slope parameter di_0/di_{rf} by considering a combination of currents,

$$i_{rf} = i_{LO} \sin \Omega \tau + i_1 \sin (N\Omega \tau + \theta), \quad (6)$$

where the signal current $i_1 \ll i_{LO}$. With the simulator we found that in the range $0 < \nu < \Omega$, the effect of i_1 is to change the current by an amount

$$\Delta i_o = - i_1 S_N \cos (\theta + \delta_N) + O(i_1^2). \quad (7)$$

(Similar changes occur in other regions of the I-V curve, but were not investigated.) Here S_N is a generalized slope parameter, with $S_1 = di_o/di_{LO}$, and $\delta_1 = 0$. With the simulator we find that all the S_N are nearly constant over the range of LO currents which reduce the zero voltage current by a factor of order 2, and $\delta_2 = 90^\circ$, $\delta_3 = 180^\circ$, etc. In Fig. 3 we show the dependence of the first few S_N on normalized frequency as determined by the simulator, for a value of LO current that reduces the critical current to $\sim 0.4 I_c$.

A rather different mode of harmonic mixing for even values of N has been observed.² When the LO current is adjusted to completely suppress the zero voltage current, efficient mixing occurs at zero dc bias. The analysis of this mode of operation requires a different approach than that presented here, so is outside the scope of the present paper.

We can now consider the combination of a LO current and a signal current which differs in frequency by a small amount Ω_{IF} from Ω_{LO} or one of its harmonics, by setting $\theta = \Omega_{IF}\tau$ in Eq. (6). Then according to (7) there is an output current i_{IF} at the difference frequency Ω_{IF} , with an amplitude $i_1 S_N$.

Since the quantity of interest is the available output power, we must consider the output impedance as well as the output current. The output impedance is the differential impedance R_D at the bias point. As is indicated in Fig. 2(b), the differential resistance between steps is practically infinite for $\Omega \leq 0.6$ when there is no noise. When noise is added, the corners of the steps are rounded and a maximum in R_D occurs midway between steps for typical values of Γ . With the simulator we find that an empirical expression for r_D midway between the zero'th and first step is:

$$r_D = P(\Gamma + \Gamma_o)^{-1/2}. \quad (8)$$

The dependence of P and Γ_o on normalized frequency is shown in Fig. 4.

When $\Gamma < \Gamma_0$ a somewhat higher value of r_D than given by (8) can be found near a step. For achievable values of Γ this is only likely to occur when $\Omega \gtrsim 1$, and throughout this paper we assume a bias at the midpoint. As can be seen from Fig. 2, the static I-V curves for a progression of LO levels are parallel. This means that the output impedance R_D will be insensitive to LO drifts for a constant-voltage biasing scheme.

It should be mentioned that in practice the differential resistance is a parameter that seems to be quite sensitive to deviations from our model caused by effects such as shunt capacitance, spurious external resonances, and various kinds of structure in the I-V curve that cannot be explained by the RSJ model. The latter includes energy gap structure, "excess current", etc. In comparing experimental results with theory it is often appropriate to treat r_D as a measured parameter. One should expect, however, that the dependence implied by Eq. (8) will be obeyed qualitatively, i.e. r_D is reduced when I_c is reduced or T is increased, etc.

The equivalent output circuit of Fig. 1(c) certainly applies in the limit of sufficiently low difference frequencies. The upper frequency limit for which it is applicable depends on the speed with which the phase evolution of the junction approaches the steady-state solution after a sudden change in i_{rf} . When the bias point is roughly midway between steps, this should occur after only a few LO cycles.¹⁰ We have directly tested the frequency dependence of the output current and impedance on a junction simulator for the case $\Gamma = 0.005$, $\Omega = 0.5$, and find that the low frequency model remains quite accurate up to $\Omega_{IF}/\Omega_{LO} = 0.1$. Even when $\Omega_{IF}/\Omega_{LO} = 0.3$, the deviation from the low frequency model is less than $\sim 20\%$.

IV. CONVERSION EFFICIENCY

An important figure of merit for mixers is the conversion efficiency, or "gain", defined as the ratio of power delivered to the IF amplifier to the available rf signal power. An expression that is applicable to any^{*} nonlinear system is

$$\eta = \left[\left(\frac{\partial I_{dc}}{\partial \sqrt{P_{LO}}} \right) \right]^2 \frac{R_D}{8} C_{IF} . \quad (9)$$

Here P_{LO} is defined as the available LO power, and C_{IF} is the coupling efficiency to the IF amplifier input impedance R_L , given by $C_{IF} = 4 R_L R_D / (R_L + R_D)^2$. In what follows we will assume that the IF amplifier is matched to the junction ($R_L = R_D$) so that $C_{IF} = 1$.

It may be argued that connecting an IF amplifier of finite input impedance to the junction violates our assumption of external current sources. It can be demonstrated, however,¹⁰ that the dc I-V curve of a junction depends only on the external impedance at frequencies of the order or greater than the Josephson oscillation frequency. Any reasonable IF amplifier coupling would be effective only at much lower frequencies; for our simulations we model the high frequency decoupling by a series inductance as is shown in Fig. 1(b).

The series resonance shown in Fig. 1(b) is the simplest representation of the rf coupling circuit that would apply to a real experiment.

^{*}For a nonlinear reactance¹⁸ Eq. (9) would not correctly predict the conversion efficiency, which is proportional to the IF frequency. The expression given is a lower limit to η for an arbitrary device.

This reflects the fact that useable Josephson junctions have a shunt resistance that is small compared to typical antenna impedances, which are of the order of several hundred ohms,¹⁹ except at particular resonant frequencies. Our simulations show that with resonant coupling of the LO, the junction response can be fairly well fit by the expression,

$$\left. \frac{\partial I_{dc}}{\partial (8P_{LO})^{1/2}} \right]_{\max} \approx \frac{S_1 R_S^{1/2}}{R_S + R_{rf}}. \quad (10)$$

Here R_{rf} , which is shown as a function of normalized frequency in Ref. 3, is a parameter that plays the role of an input resistance at the rf frequency. The expression for conversion efficiency then becomes

$$\eta = \frac{S_1^2 R_S R_D}{(R_S + R_{rf})^2}. \quad (11)$$

Optimization of η by varying R_S is complicated by the fact that when R_S is of the order of R the differential resistance R_D can be strongly reduced from the value given by Eq. (8). This effect is particularly pronounced for small Ω . Thus the value of R_S for which η is maximum is greater than R_{rf} . This somewhat disturbing result occurs because a Josephson junction does not behave as a simple two-port device. Its properties are affected by the impedance it sees not only at the input and output frequencies, but at many other frequencies as well. When the noise performance is considered, the optimum value of R_S can be still larger. Hence the parameter R_{rf} is of little significance in establishing the optimum source resistance. We put off a detailed discussion of these

effects of strong coupling to a later section, and consider the current-driven limit $R_S \gg R$. Then Eq. (11) becomes

$$\eta \approx S_1^2 \frac{r_D}{r_S}, \quad r_S \gg 1. \quad (12)$$

In the expression (12) for conversion efficiency there is an implicit dependence on the noise parameter Γ via the factor r_D . We have demonstrated with the simulator that S_1 is independent of Γ . Although the values of S_N for $N > 1$ were obtained with $\Gamma = 0$ it is plausible that they too are independent of Γ . The dependence of conversion efficiency on junction parameters for a given normalized frequency and rf coupling, $\eta \sim \Gamma^{-1/2} \sim (I_c/T)^{1/2}$, suggests that I_c should be large. Since the RI_c product is roughly constant, this conflicts with a practical requirement of microwave matching, that R should not be < 10 ohm.

For the case of harmonic mixing ($\Omega_{sig} \approx N\Omega_{LO}$, $N > 1$), the conversion efficiency is given by Eq. (12) with S_1 replaced by S_N . It is some interest to compare the expected mixing efficiency for various orders keeping the signal frequency fixed, i.e. using a LO frequency near Ω_{sig} , $\Omega_{sig}/2$, $\Omega_{sig}/3$, etc. In Fig. 5 we plot $S_N^2 r_D$, which is proportional to the conversion efficiency, as a function of Ω_{sig} and N . Note that S_N and r_D are evaluated at Ω_{sig}/N . We have assumed $\Gamma = 0.005$, as would result for instance if $T = 4.2$ K, $I_c = 35$ μ A. The precipitous decline in conversion efficiency for the fundamental mixing case above $\Omega \sim 0.6$ is somewhat exaggerated due to the assumption of a bias point midway between the zeroth and first steps. In fact, a bias point with higher r_D can usually be found closer to one of the steps. This becomes increasingly true for $\Omega > 1$.

In a recent experiment by D'yakov et al.²⁰ on point contact Josephson junctions poorly coupled to the microwave source (and thus satisfying the criterion of being current-driven) the observed fall off with harmonic order was much slower than indicated in Fig. 5. We find that most of the discrepancy comes from deviations in the experimental values of r_D from the predictions of the resistive model. The observed values of the ratio S_3/S_1 were generally somewhat greater than our prediction, in some cases by as much as 35%.

The fact that Josephson effect mixers require very little LO power means that it should usually be possible to derive adequate power for fundamental mixing from conventional sources using diode harmonic generators. It therefore seems that it would be worthwhile to make use of the relatively efficient harmonic mixing capabilities of the Josephson device only for special applications such as frequency comparison,^{21,22} etc.

V. MIXER NOISE

The second important figure of merit for a mixer is its single side-band noise temperature T_m . We obtain this quantity by first computing an output noise temperature T_{out} which is related to T_m by $T_m = T_{out}/\eta$. To predict the output noise we need a model for the equivalent driving noise current i_n of Eq. (5). We consider an expression that was first given by Scalapino²³ for tunnel junctions:

$$I_n^2(\nu) = eB \left[I_q \left(V + \frac{h\nu}{e} \right) \coth \frac{eV + h\nu}{2kT} + I_q \left(V - \frac{h\nu}{e} \right) \coth \frac{eV - h\nu}{2kT} \right]. \quad (13)$$

Here ν is the frequency at which the noise is observed, B is the bandwidth, and $I_q(\nu)$ is the quasiparticle current in the junction at a bias voltage V . When I_q is proportional to V , as is assumed in the RSJ model, the above expression reduces to

$$I_n^2(\nu) \approx \frac{2EB}{R} \quad (14)$$

where E is the largest of eV , $h\nu$, or $2kT$. We will identify the regimes corresponding to the first, second, or third term being dominant as shot noise, photon noise, or thermal noise, respectively. Almost all discussions in the literature of noise effects in the RSJ model have assumed the thermal noise limit. The parameter Γ evaluated at the physical temperature T characterizes the driving noise amplitude for this case.

In general, the driving noise is processed by various nonlinear interactions within the junction to produce a low frequency voltage noise that is greater than $R_D^2 I_n^2(0)$. Likharev and Semenov²⁴ calculated the voltage noise response to a driving current noise I_n for the RSJ model without rf bias:

$$V_n^2(0) = R_D^2 \left[I_n^2(0) + I_n^2(2eV/h)/2i^2 \right], \quad (15)$$

where i is the normalized bias current. This expression is valid as long as noise rounding is not severe.

Experimental results for the voltage noise across point contacts without rf bias are not consistent. Kanter and Vernon²⁵ observed noise at ~ 150 KHz, and the data presented are considerably in excess of Eq. (15),

especially at low bias voltage. They note, however, that some junctions showed a dependence on voltage that is qualitatively similar to Eq. (15). Insufficient information is given about these junctions to make quantitative comparisons. Noise measurements in our laboratory on oxidized Nb point contacts at $\sim 50 \text{ MHz}$ ⁴ are in qualitative agreement with Eq. (15),* but quantitatively in excess by approximately a factor 2.

Measurements of the linewidth of the Josephson oscillation, which should be proportional to the low frequency voltage noise, have been made both directly²⁶ and indirectly²⁷ in point contacts. At high bias voltages these results scale as would be expected from Eq. (15) in the appropriate shot noise limit, but with a magnitude a factor 2 or so too high. At low voltages the noise is much higher than given by Eq. (15).

The results of some of the experiments mentioned above were compared with an expression derived by Stephen²⁸ for the voltage noise across a tunnel junction biased on a cavity mode step. Whatever agreement was observed would seem to be fortuituous, since the model used for Stephen's calculation does not apply to point contacts. A certain amount of confusion has resulted from the identification of one of the terms in Stephen's expression as "pair shot noise". In fact, this term arises as a result of detection in the Josephson junction of photon fluctuations in the cavity, rather than intrinsic fluctuations in the pair current.

As we have defined it, shot noise in junctions for which the RSJ model applies may be considerably reduced from the value given by Eq. (13). Full shot noise is expected when the voltage drop occurs across a region much smaller than an electron mean free path,²⁹ as is the case for tunnel

*Including corrections that arise when noise-rounding is severe.

junctions. For many low-capacitance structures, such as the variable-thickness bridge, however, this may not be the case.

There exist no analytic expressions in the literature for the low frequency noise output from a Josephson junction biased for optimum mixer operation. We have used the analog simulator to determine the output noise when it is driven with an appropriate noise current, for a variety of junction parameters. Since at least some of the available experimental data are consistent with calculations based on Eq. (14) as the correct driving noise, we have used this expression in the simulator calculations with the philosophy that the results should represent a lower limit on the noise in a junction.

There are two extreme limits that can be considered: purely thermal noise ($2kT \gg h\nu_{LO}$) and purely photon noise ($h\nu_{LO} \gg 2kT$). These correspond to a white driving noise spectrum and a spectral density proportional to frequency (blue noise), respectively. Both extremes are likely to be encountered in practical experiments. We note that the crossover between regimes occurs at a frequency $\nu_{LO} = 42$ GHz when $T = 1$ K.

For the simulations, the white noise current was obtained by amplifying the Johnson noise in a resistor using a low-noise amplifier (PAR 185). This could be converted to "blue noise" by passing it through a linear network with a frequency response which varied as $\sim \nu^{\frac{1}{2}}$.

In the mixer application the presence or absence of shot noise is largely irrelevant: In the thermal noise limit, we have $2kT \gg eV$, since $eV \sim h\nu_{LO}/4$ at the optimum bias point. In the photon noise dominated region, the shot noise contribution is important only for frequencies less than $\nu_{LO}/4$. We shall show that noise currents in this range contribute little to the output noise.

We first consider the case of thermal noise. In this limit the junction is driven by white noise with a spectral density given in normalized units by $i_n^2 = \frac{2}{\pi} \Gamma \Delta \Omega$. The spectral density of the output voltage noise V_n from a junction simulator was determined with the aid of a digital computer system, up to a frequency $\nu_{LO}/10$ for various values of important parameters.

It is most convenient to consider the output noise current I_{no} as is indicated in the equivalent circuit of Fig. 1(c), rather than the noise voltage. We define a noise parameter β^2 as the ratio of I_{no}^2 to the driving noise current I_n^2 at low frequencies:

$$\beta^2 \equiv \frac{I_{no}^2(0)}{I_n^2(0)} = \frac{V_n^2(0) R}{4kT R_D B} . \quad (16)$$

Fig. 6 shows some simulator predictions of β^2 as a function of bias voltage for a junction biased with an rf current source whose amplitude is appropriate for optimum mixer operation.

To determine the mixer noise temperature we note that the effective output temperature is $T_{out} = \beta^2 r_D T$, where T is the physical temperature of the junction. Then

$$T_m = T_{out} / \eta = \beta^2 T r_S / S_1^2 , \quad (17)$$

where we have used Eq. (12) for η . The only term in this expression that depends on bias voltage (if the voltage is below the first step) is β^2 . The minimum seen in Fig. 6 to occur midway between the zeroth and first

steps is a feature observed for all Ω and for all values of Γ small enough to leave some step structure visible in the I-V curve. Hence the bias point for optimum mixer noise temperature coincides with the point of maximum conversion efficiency when $\Omega \leq 1$. We have not studied the case of higher normalized frequencies, where the optimum in conversion efficiency can lie closer to the zeroth step.

The simulations show that β_{\min}^2 is independent of Γ (for a given Ω), as long as Γ is small enough to leave $r_D \gtrsim 1$. It is also unchanged over the range of LO levels appropriate for mixer operation, i.e. those that suppress the critical current by 50-80%. Hence β_{\min}^2 is a function only of normalized frequency. This dependence is shown in Fig. 7. We also show β_{\min}^2/S_1^2 , which according to Eq. (17) should be proportional to the mixer noise temperature in the current-biased limit. This factor is practically independent of normalized frequency over most of the range of interest to us. Note that T_m does not depend on Γ , in contrast to the conversion efficiency. This simplification unfortunately does not apply in the case of a strongly coupled junction ($r_S \sim 1$), as we shall show in a later section.

Eq. (17) is valid in the current-biased limit, $r_S \gg 1$. On the basis of simulations with $r_S \leq 2$ to be described in section VII, we can guess that (17) remains fairly accurate with r_S as low as ~ 4 . Using this value along with the results given in Fig. 7, we find $T_m \lesssim 40$ K for Ω in the range 0.1 - 0.9. To make a similar estimate of conversion efficiency, we must specify Γ . According to Fig. 5, $\eta > 0.25$ in the above range of frequencies if $\Gamma \leq 0.005$. The latter condition would be met, for example, if $I_c > 35$ μ A at $T = 4$ K.

Equation (17) suggests that T_m can be improved indefinitely by lowering the junction temperature T . However, once $T \lesssim h\nu_{LO}/2k$ the thermal noise results no longer apply. To investigate the low temperature regime, we have driven the simulator with "blue" noise - i.e. with a current spectrum given by $I_n^2(\nu) = 2h\nu B/R$. According to Eq. (13), this corresponds to the limit $T = 0$. In analogy to the definition for β^2 , a dimensionless output noise parameter can be defined:

$$\gamma^2 = I_{no}^2(0)/I_n^2(\nu_{LO}) . \quad (18)$$

We find again that as long as $r_D > 1$ this parameter is independent of R . Its dependence on normalized frequency is shown in Fig. 7. An expression can then be obtained for the mixer noise temperature in the limit $T \rightarrow 0$ which is analogous to Eq. (17),

$$T_m = \frac{\gamma^2 r_S}{S_1^2} \frac{h\nu_{LO}}{2k} . \quad (19)$$

Since γ^2 is of the same order as β_{min}^2 over much of the range of normalized frequency being studied here, we can roughly say that in the low temperature limit the junction is at an effective ambient temperature $h\nu_{LO}/2k$.

It is interesting to speculate on the mechanisms giving rise to an equivalent output noise current near zero frequency greater than the driving noise. One obvious source of the extra noise is down-conversion of high frequency noise components due to the fundamental and harmonic mixing processes we have discussed. This should contribute an amount

$2 \sum_{N=1}^{\infty} S_N^2$ to β^2 , and $2 \sum_{N=1}^{\infty} NS_N^2$ to γ^2 , respectively. The factor 2 arises from the fact that two sidebands at each frequency are down-converted into the IF bandwidth. We find in fact that the above sums are close to half of the directly calculated values of $\beta^2 - 1$ and γ^2 , respectively. We have been advised³⁰ that the remaining noise can be accounted for by processes analogous to mixing with the Josephson oscillation in junctions with no rf bias.²⁴

VI. SATURATION

For any mixer the conversion efficiency will become nonlinear for signal powers approaching some fraction of the L0 power. In a Josephson effect mixer the L0 level is sufficiently small that such saturation effects could severely limit its usefulness in some applications. In this section we consider two mechanisms for saturation.

One mechanism for nonlinear response corresponds to output voltage excursions that exceed the range of constant differential resistance on the I-V curve. Considering the qualitative I-V curves shown in Fig. 2, it is clear that when the peak-to-peak voltage excursions approach $h\nu_{L0}/2e$ the junction will be strongly saturated.³¹ More generally, we propose that saturation occurs when the rms IF voltage exceeds $x \cdot h\nu_{L0}/2e$, where x lies in the range 0.1 - 0.2, depending on the stringency of the criterion for saturation as well as details of the I-V curves. The corresponding signal power is

$$P_{\text{sat}} = x^2 \left(\frac{h\nu_{\text{LO}}}{2e} \right)^2 / R_D = \frac{x^2 \Omega^2 r_S}{S_1^2 r_D^2} \cdot RI_c^2. \quad (20)$$

In Ref. 32 data are shown suggesting that the saturation power scales as RI_c^2 . According to the above equation this is true for fixed Ω , r_D , and rf coupling. As all of these parameters were not recorded, we cannot make a detailed comparison with Eq. (20). If we assume $r_S \sim 1$, as was typical of the experiments of Ref. 32, the two examples shown (Fig. 27) give $x = 0.23$ and $x = 0.33$, respectively, for 1 dB gain compression. If Eq. (8) is used for r_D , with $\Gamma \gg \Gamma_0$, Eq. (20) becomes

$$P_{\text{sat}} = \frac{2\pi x^2 \Omega r_S}{S_1^2 P^2} \cdot kT_{\text{VLO}} \gtrsim 50 x^2 r_S kT_{\text{VLO}}. \quad (21)$$

The numerical factor is valid for normalized frequencies in the range 0.1 - 1.0.

A second saturation mechanism is applicable to the frequently encountered situation where the "signal" is in fact noise, e.g. when a radiometer is used to observe the temperature T_S of a black-body source which is coupled over a bandwidth B to the mixer. In the limit of current-source coupling that is being considered here, we can say that the effective junction temperature is $T + T_S/r_S$ within the coupling bandwidth, and T over the remaining frequency region. The differential resistance of the junction will depend on T_S in a manner somewhat similar to its dependence on T and, since the conversion efficiency is proportional to r_D , the mixer will have a nonlinear response to changes in T_S .

To estimate the magnitude of this effect, we use a generalization of Eq. (8) for the differential resistance:

$$r_D^{-2} = \frac{\Gamma + \Gamma_o}{P^2} + \left(\frac{B}{v_{LO}} \right) \cdot \frac{\Gamma_S}{Q^2}. \quad (22)$$

Here B is the bandwidth over which the source is coupled to the junction, and $\Gamma_S = 2ekT_S/\hbar I_c r_S$. The dependence implied by Eq. (22) was verified for $\Gamma = 0$ with the simulator, but not for the general case $\Gamma \neq 0$, $\Gamma_S \neq 0$. The dependence of Q on normalized frequency is shown in Fig. 4. In the radiometer mode one looks for small changes in the output power P_{out} of the IF amplifier corresponding to changes in the source temperature. Suppose in particular the temperature of the source changes from zero to some value T_S . Then we have

$$\Delta P_{out} \propto r_D(T_S)(T_m + 2T_S) - r_D(0)T_m. \quad (23)$$

This equation assumes that β^2 , S_1^2 , C_{IF} , and T_{IF} are constant, a reasonable assumption if the IF amplifier is initially matched to the junction. The factor 2 in the parentheses results from the fact that two sidebands are down-converted into the IF bandwidth. Setting $\Gamma_o = 0$ for simplicity, we have

$$r_D \propto (T + \epsilon T_S)^{-1/2},$$

$$\text{where } \epsilon = \frac{P^2}{Q^2} \left(\frac{B}{v_{LO}} \right) \frac{1}{r_S}. \quad (24)$$

As can be seen in Fig. 4, $(P/Q)^2$ is virtually independent of normalized frequency and has a maximum value ~ 0.45 . It can be shown that to lowest order in ϵ Eq. (23) becomes

$$\Delta P_{\text{out}} \propto r_D(0) \left[\left(2 - \frac{\epsilon T_m}{2T} \right) T_S - \frac{\epsilon T_S^2}{2T} \right]. \quad (25)$$

There are two results of the modulation of r_D by the source temperature: The effective conversion efficiency is reduced from what it would be for a coherent signal, and there is a square law (detection) contribution to the IF response. The relative change in conversion efficiency is

$$\frac{1}{4} \left(\frac{B}{v_{LO}} \right) \frac{\beta^2 P^2}{S_1^2 Q^2} \lesssim \left(\frac{B}{v_{LO}} \right), \quad (26)$$

where we have used Eq. (17) for T_m . The requirement that this quantity be small places a fairly stringent requirement on the allowable coupling bandwidth. If the bandwidth is narrow enough that the conversion efficiency is not significantly altered, the amount of "signal" power that will result in a 1 dB gain compression due to the square law term in (25) is

$$P_{\text{sat}} \approx 0.2k \left(\frac{4T}{\epsilon} \right) B \approx 2r_S k T v_{LO}. \quad (27)$$

In practice, care is required to avoid confusion of these effects with linear mixing. Comparing with the expression for output saturation, Eq. (21), we see that if we choose $x = 0.2$, the two mechanisms are of roughly equal importance in determining a saturation power. If $r_S = 4$

and $T = 4$ K, Eq. (27) shows that a relative coupling bandwidth of 10% to a 300 K source is sufficient to compress the gain by 1 dB.

VII. STRONGLY COUPLED JUNCTIONS

We now consider the case of strong rf coupling, i.e. where the source resistance R_S is of the same order as the junction resistance. When there are no reactive elements and the source is perfectly coupled over the complete bandwidth from dc to (at least) the gap frequency, the problem can be cast into the form of a current-biased, resistively shunted junction.³² Not only is such a circuit impossible to realize in practice but, in view of the discussion in the last section, saturation effects could be expected to dominate. We have chosen to investigate the series-resonant equivalent circuit shown in Fig. 2(b) to represent the microwave coupling scheme.

The added complexity of such a circuit shows itself in the appearance of hysteresis in the static I-V curve at bias points appropriate for mixer operation when R_S is of the order of the junction resistance. An explanation for the instability of a bias point between the zero'th and first steps is given in section VIII. As might be expected, the addition of noise can result in a "smearing out" of the hysteretic region to give

a single-valued dc I-V curve. This is well known for the case of capacitively caused hysteresis.³³ In Fig. 8 we show a sequence of I-V curves with various values of the noise parameter Γ , obtained with a simulation of the full circuit of Fig. 2(b). It is noteworthy that once the noise is large enough to suppress the hysteresis, the differential resistance between the zero'th and first steps is significantly less than it would be for the current-driven case. This is especially pronounced at low normalized frequencies, where the reduction in r_D can be as much as an order of magnitude in the well coupled case.

Another characteristic of the I-V curves of strongly coupled junctions is a pronounced effect on the shape when the LO frequency is detuned from the center frequency of the resonant circuit. An example of this is given in Fig. 9. Note that by operating somewhat off resonance the differential resistance can be increased above the value at resonance. The complicated dependence of r_D on source resistance, tuning, etc., makes it impossible to arrive at a simple analytical expression for conversion efficiency in the strong coupling range.

A second and more important effect of strong coupling of the LO is

an increase in β_{\min}^2 over the value observed for current-source coupling. The excess can be an order of magnitude for typical experimental parameters. In general, β_{\min}^2 increases as Γ decreases, becoming divergent as $r_D \rightarrow \infty$. Excess noise of this sort seems to be a general feature of hysteretic I-V curves that have been smeared by thermal noise into continuous ones, no matter what is the mechanism for hysteresis. The existence of extra low frequency noise seems quite plausible if the smearing process is regarded as one in which the thermal noise randomly drives the junction between its two stable states.

Since the properties of strongly coupled junctions depend on many parameters, such as Γ and the tuning of the resonant circuit, that do not enter in the current-driven case, it is very difficult to make general predictions of the performance to be expected. In previous treatments³⁴ we have simply assumed that the noise with strong coupling is a factor 2 or so worse than with current source coupling. In fact, the discrepancy can be much worse. We have recently obtained simulator predictions of mixing performance under a variety of conditions of strong coupling that might typically be used. These results, which are summarized in Fig. 10, are fairly sensitive to details of the model. Addition of a small shunt capacitance or a more realistic modelling of the rf circuit, for instance, might have a substantial effect. They should not be taken as exact numerical predictions, but as indications of general trends.

One of the most significant predictions is the rapid deterioration in T_m when I_c is increased, but the RI_c product is held fixed. This reflects the fact that β_{\min}^2 depends on Γ , in contrast to the current-biased limit. In a mixer utilizing a low resistance Josephson structure

such as a thin film weak link, the microwave circuit should be designed for fairly weak coupling ($r_s \gtrsim 4$, say). On the other hand, if the resistance is high enough there may be some advantage in reducing r_s to 1 or 2. Note that it is almost never useful to make $r_s < 1$. Another difference from the weakly coupled limit is a weaker dependence of T_m on the junction temperature. We have noted for the former case that $T_m \propto T$ for $T \gtrsim h\nu_{LO}/2k$. For strongly coupled junctions a temperature can generally be reached below which no improvement is possible, even if it is still in the thermal noise limit.

We have also considered the photon noise dominated limit for one set of parameters of a strongly coupled junction. We find that the results for conversion efficiency and noise are the same as if it were driven by white noise corresponding to $\Gamma = 2\pi e\nu_{LO}/I_c$. If this holds true generally we can use the predictions of Fig. 10 in the high frequency limit $h\nu_{LO} > 2kT$ by considering the junction to be at an effective temperature $h\nu_{LO}/2k$.

In the above discussion of parameter optimization we have ignored the variation of conversion efficiency on the grounds that it is in every case large enough that a state-of-the-art IF amplifier will not contribute significantly to the system noise temperature. To obtain values of conversion efficiency significantly greater than the value 0.3 which is potentially available from Schottky diode mixers, an increase in I_c with a corresponding sacrifice in T_m is necessary. Note that there is no fundamental principle prohibiting values of η greater than unity - the IF power is derived from the bias supply rather than the signal.

From Fig. 9 it is seen that r_D can be substantially increased by

detuning the circuit resonance slightly. In this case we should replace the denominator of Eq. (11) by $(R_S + R_{rf})^2 + X^2$, where X is the external reactance introduced. The increase in r_D can offset the increase in the denominator due to finite X , and yield improved conversion efficiency. However, the mixer noise temperature is invariably degraded by such detuning, so that an overall system noise improvement will result only if the IF amplifier noise contribution is significant.

The values of β_{\min}^2 used in preparing Fig. 10 were measured near zero IF frequency. Our noise-measuring system can be used to determine the noise spectrum for frequencies as large as $\nu_{LO}/10$. In contrast to the current-driven case, we generally observe some frequency dependence of the output noise for strongly coupled junctions. For IF frequencies within the coupling bandwidth, β_{\min}^2 rarely varies by more than a factor of 2 and most often increases with increasing frequency. This means that the high IF frequencies which are often used in Schottky diode heterodyne systems should not be necessary with Josephson mixers.

VIII. ARRAYS OF JUNCTIONS

It has been suggested³⁵ that the problem of impedance matching to the low resistance of presently available thin film bridge junctions⁸ can be alleviated by using series arrays of such devices. In the current-driven limit, it can be shown that neither the conversion efficiency nor the noise performance of such an array is improved over what can be achieved (in principle) with a single junction. The impedance matching

difficulties, however, are removed at both the signal and the IF frequency. In this respect, use of an array is equivalent to impedance transforming a single junction. One exception to this equivalence is the saturation power of an array, which increases linearly with the number of junctions.

It is interesting to speculate whether the excess noise due to hysteresis effects in the strong coupling limit would still exist in arrays. It can be argued³⁵ that even when the array is collectively well coupled to an rf source, the individual junctions are presented with an external impedance much greater than their own resistance, and so are effectively current biased.

To examine this idea, we propose a simple mechanism to explain the instability of a bias point between steps for a strongly coupled single junction: We have found, in agreement with a previous study,³⁶ that the impedance at the LO frequency of a current-biased junction always decreases with increasing bias voltage. With a finite LO source impedance, it follows that the LO current must increase with increasing voltage bias. However, an increase of LO current will further suppress the critical current. The overall result in the absence of noise is a dc negative resistance, which prevents a stable bias. It appears that this mechanism should apply equally to an array of junctions. Unlike the case of a single junction, however, the thermal noise in the junctions is not expected to have a significant smearing effect on the overall I-V characteristic of an array. Hence the negative resistance will persist even for fairly large values of Γ . The problems with strong coupling to an array will probably involve achievement of a stable bias rather than excess noise.

The junctions in an array must be sufficiently alike in their properties that most of them can be biased near the optimum voltage $\approx h\nu_{LO}/4e$. If we assume that the fabrication technique results in junctions with some spread in I_c but uniform values of RI_c , the variation in bias voltage $\langle \delta V \rangle$ of an individual junction from the average $\langle V \rangle = h\nu_{LO}/4e$ is given by:

$$\delta V = R_D \left(\frac{I_o}{I_c} + \frac{S_1 I_{rf}}{I_c} \right) \delta I_c . \quad (28)$$

Here δI_c is the deviation of the critical current of the junction from the average, and I_o and I_{rf} are the dc bias current and rf current, common to all the junctions. The term in parentheses is close to unity for optimum bias conditions at all values of normalized frequency. If we compute R_D from Eq. (8) with $I_c = 100 \mu A$, $T = 4.2 K$, $\Omega = 0.5$, we find $\delta V / \langle V \rangle \approx 40 \delta I / I_c$. Hence only those junctions in an array whose critical currents are within $\sim 1\%$ of the average will contribute an appreciable IF voltage.

IX. REAL JUNCTIONS

The theory developed in this paper is relevant to real junctions only to the extent that they are described by the resistively shunted junction model. The earliest theoretical justification for this model was supplied by Aslamazov and Larkin⁷ for the case of a three-dimensional constriction joining two bulk superconducting regions. If the characteristic dimension a of the constriction satisfies the constraint $\ell \ll a \ll \xi$ (ℓ is the electron mean free path, ξ is the coherence length), the Ginzberg-Landau (GL) equations predict a sinusoidal static current-phase relation, with the critical current being related to the normal resistance R of the constriction by Eq. (1). Likharev and Yakobson³⁷ have extended these calculations to the case of a thin filament of arbitrary length connecting

two bulk pieces of superconductor. They find that as long as the length of the bridge is less than \sim twice the coherence length, the current-phase-relation does not differ by more than \sim 20% from sinusoidal, and the RI_c product can actually exceed the tunnel junction limit by \sim 30%.

According to the RSJ model, voltage spikes with a width $\sim \tau_J = \hbar / (2eRI_c)$ will occur under virtually any bias condition involving a dc voltage component. The foregoing analyses might not be expected to be valid unless the GL order parameter can respond at least as rapidly as the voltage across the junction varies. In fact, the order parameter relaxation time is predicted to be from \sim 6-12 times greater than τ_J in those instances where a time-dependent GL equation can be derived from the microscopic theory of superconductivity. Recently Likharev and Yakobson³⁸ and Baratoff and Kramer³⁹ obtained solutions to the time-dependent equations for the case of the thin filament joining two superconductors. For sufficiently short lengths, it is found that the RSJ model is recovered with corrections that amount to a small change in the effective normal resistance and a $\cos \phi$ modulated conductance.

It is possible that the dimensional requirements for validity of the RSJ model might be met in point contacts, at least if the bias voltage is not too large. However, with the dimensions that can reasonably be expected to be achievable for film type bridges (length comparable to the coherence length) deviations from the RSJ model are apparent in the calculations. For example, the voltage oscillations are smaller in amplitude and somewhat skewed. The resemblance is still strong enough that one might expect the RSJ model predictions of mixing, with an "effective", smaller, critical current, to be useful.

The time-dependent GL theory does predict one very common observation in point contacts and bridge structures: the offset voltage (or current) that persists up to very high bias currents. On the other hand, it cannot account for the gap structure that is frequently seen in these structures.

Recently small area tunnel junctions with very high current density have been reported⁴⁰ to have I-V curves showing very little hysteresis, presumably because β_c is sufficiently small. McDonald *et al.*⁴¹ have reported the results of calculations based on the tunneling formalism in the limit of small capacitance. It has been proposed²⁹ that this model should apply also to high resistance point contacts whose contact area is smaller than an electron mean free path. The calculated I-V curves show significant gap structure, as well as a much greater sensitivity to β_c than is characteristic of the RSJ model. It is plausible that, with a small amount of noise rounding, single-valued I-V curves would result, making such junctions useable as mixers. It would be of considerable interest to extend these calculations to the case of a low capacitance tunnel junction biased with an rf current source, allowing comparison with the predictions of the RSJ model.

Another feature of real junctions that has not been accounted for in our analysis is the effect of self-heating. This has recently been addressed by Tinkham *et al.*⁴² for the case of a superconducting constriction. He obtains a rather general expression for the maximum temperature in the bridge:

$$T' = \left[T^2 + 3 \left(\frac{eV}{2\pi k} \right)^2 \right]^{1/2}. \quad (29)$$

We might guess that the effective junction temperature is the average of T' and the ambient temperature T . Assuming a bias point $V = h\nu/4e$ for mixer operation, it is easily demonstrated that quantum noise effects will outweigh the increase in temperature implied by Eq. (29).

A much more important effect of self-heating is a suppression of the critical current. Tinkham et al. estimated this effect by using the time-independent GL equations with a spatially varying temperature. They found $I_c \sim \exp(-P/P_0)$, where P is the power dissipated in the junction and P_0 is a parameter that depends only on materials parameters of the superconductor and bridge geometry,

$$P_0 \sim T_c^2 \xi(0)/\rho . \quad (30)$$

Here ρ is the resistivity of the metal. Numerically, it is found that for most pure superconductors $P_0 \approx 10 \mu W$.

We can estimate the consequence of self-heating on I-V curves by supposing that at finite voltage the RSJ model is obeyed with a critical current which depends on the power dissipation in the junction. This leads to hysteretic I-V curves, with the amount of hysteresis being determined by $\delta \equiv RI_c^2/P_0$. The amount of hysteresis ΔI between the zeroth and first steps for a junction biased with an rf current can be calculated to first order in δ using published dependences of step heights for the RSJ model.^{15,16,17} If the rf current suppresses I_c by 50% in the absence of self-heating, we find

$$\Delta I < 0.45 I_c \Omega \delta \quad (31)$$

for $0.1 < \Omega < 1.0$. For most experimental conditions a fractional hysteresis $\Delta I/I_c = 0.02$ would be so thoroughly masked by noise as to be unimportant. At $\Omega = 0.3$ this would require $\delta < 0.15$. Using the value $P_0 = 10 \mu W$, and assuming an RI_c product of 1 mV, we find that heating effects are unimportant if $R > 0.7 \text{ ohm}$. Empirically determined values of P_0 for point contacts more often lie in the range 1-3 μW , which still presents no serious limitation for practical mixers. However, the use of alloys is certainly precluded from this point of view, since Eq. (30) implies a dependence $\ell^{-3/2}$ on the electron mean free path.

CONCLUSION

We have found that the RSJ model predictions of mixing performance fall naturally into two regimes: weak and strong coupling to the signal source. In the former case the predictions take a particularly simple form. It is found that the mixer noise temperature is roughly independent of normalized frequency if $0.1 < \Omega < 1.0$, and scales linearly with the (actual or effective) junction temperature.

The weak coupling limit will probably apply in most experiments involving the high end of the frequency range we have considered if only because of practical limitations. Our results predict quite respectable performance nonetheless. For instance, at 300 GHz ($T_{\text{eff}} \approx 7 \text{ K}$) with $r_s = 4$, we would have $T_m \approx 300 \text{ K}$ using a junction whose RI_c product exceeds 600 μV . The conversion efficiency would be as good as the best that could be expected from a Schottky mixer.

At lower frequencies where strong coupling could in principle be achieved, the complexity of the observed behavior in our simulations precludes definite predictions. The main overall conclusion to be drawn is that for a fixed RI_c product the normal resistance should be as large as possible - i.e., noise rounding should be pronounced. This is in contrast to the weakly coupled case, where all that matters in determining T_m is the ratio of junction and source resistances. The simulated results in the strong-coupled case are probably more sensitive to small deviations from the RSJ model than those for the weak-coupled case. In particular, the general lowering of r_D that is implied in the common observation of "excess current" could result in a lower threshold in R_S for the appearance of hysteresis. This in turn could reduce the excess noise in the junction, resulting in a lower noise temperature than our simulations would predict.

Finally, we emphasize the practical importance of saturation effects in Josephson mixers. In most applications the bandwidth in which the mixer is coupled will have to be restricted. The microwave coupling circuit could, of course, also function as a filter. Indeed, an advantage of using low resistance junctions is that the impedance transformation required, if done resonantly, necessarily implies a narrow coupling bandwidth. Only with large arrays is the saturation level high enough to permit broad band coupling.

ACKNOWLEDGEMENTS

The authors wish to acknowledge many useful conversations with Y. Taur, and to thank K. Andriesse and S. Weinreb for critical readings of the manuscript. We also thank R. Bailey for assistance in the use of his computer noise analysis system.

REFERENCES

* Research supported by the U. S. Office of Naval Research.

† Present address: Naval Research Laboratory, Washington, D. C. 20375.

1. C. C. Grimes and Sidney Shapiro, Phys. Rev. 169, 397 (1968).
2. Y. Taur, J. H. Claassen, and P. L. Richards, Rev. Phys. Appl. 9, 261 (1974).
3. Y. Taur, J. H. Claassen, and P. L. Richards, Appl. Phys. Lett. 24, 101 (1974).
4. J. H. Claassen, Y. Taur, and P. L. Richards, Appl. Phys. Lett. 25, 759 (1974).
5. B. D. Josephson, Phys. Letters 1, 251 (1962); Advan. Phys. 14, 419 (1965).
6. V. Ambegaokar and A. Baratoff, Phys. Rev. Lett. 10, 486 (1963); 11, 104 (1963).
7. L. G. Aslamazov and A. I. Larkin, Zh. ETF Pis. Red. 9, 150 (1969) [JETP Lett. 9, 87 (1969)].
8. M. T. Levinson, Rev. Phys. Appl. 9, 135 (1974).
9. L. Solymar, Superconductive Tunneling and Applications (Chapman and Hall, London, 1972).
10. A. N. Vystavkin, V. N. Gubankov, L. S. Kuzmin, K. K. Likharev, V. V. Migulin, and V. K. Semenov, Rev. Phys. Appl. 9, 79 (1974).
11. C. A. Hamilton, Rev. Sci. Instr. 43, 445 (1972).
12. C. K. Bak, Rev. Phys. Appl. 9, 25 (1974).
13. D. E. McCumber, J. Appl. Phys. 39, 3113 (1968); W. C. Stewart, Appl. Phys. Lett. 12, 277 (1968).
14. M. T. Levinson and B. T. Ulrich, IEEE Trans. Mag. MAG-11, 807 (1975).
15. P. Russer, J. Appl. Phys. 43, 2008 (1972).

16. H. Fack and V. Kose, J. Appl. Phys. 42, 320 (1971).
17. C. A. Hamilton, J. Appl. Phys. 44, 2371 (1973).
18. J. M. Manley and H. E. Rowe, Proc. IRE 44, 906 (1956).
19. S. A. Schelkunoff, Proc. IRE 29, 493 (1941).
20. V. P. D'yakov, V. N. Gubankov, A. M. Spitzin, and A. N. Vistavkin, IEEE Trans. Mag. MAG-13, 237 (1977).
21. T. Blaney and D. J. E. Knight, J. Phys. D7, 1882 (1973).
22. D. G. McDonald, A. S. Risley, J. D. Cupp, K. M. Evenson, and J. R. Ashley, Appl. Phys. Lett. 20, 296 (1972).
23. D. J. Scalapino, Proc. of the Symposium on the Physics of Superconducting Devices (Univ. of Virginia, Charlottesville), 1967.
24. K. K. Likharev and V. K. Semenov, JETP Lett. 15, 442 (1972).
25. H. Kanter and F. L. Vernon, Phys. Rev. Lett. 25, 588 (1970).
26. G. Vernet and R. Adde, Appl. Phys. Lett. 19, 195 (1971).
27. G. Vernet, J.-C. Henaux, and R. Adde, preprint.
28. M. J. Stephen, Phys. Rev. 182, 531 (1969).
29. K. K. Likharev, private communication.
30. Y. Taur, private communication.
31. T. Blaney and D. J. E. Knight, J. Phys. D6, 936 (1973).
32. Y. Taur, Ph.D. Thesis, 1974.
33. J. Kurkijärvi and V. Ambegaokar, Phys. Lett. 31A, 314 (1970).
34. P. L. Richards, J. H. Claassen, and Y. Taur, Proc. 14th Intern'l Conf. on Low Temp. Phys., M. Krusius and M. Vuorio, Eds., Vol. 4, p. 238 (American Elsevier, New York, 1975).
35. P. L. Richards, SQUID - Superconducting Quantum Interference Devices and Their Applications, H. D. Hahlbohm and H. Lübbig, Eds. (Walter de Gruyter, Berlin - New York, 1977).

36. F. Auracher, J. Appl. Phys. 44, 848 (1973); L. G. Aslamazov and A. I. Larkin, JETP Lett. 9, 87 (1969).
37. K. K. Likharev and L. A. Yakobson, Sov. Phys. - Tech. Phys. 20, 950 (1976).
38. K. K. Likharev and L. A. Yakobson, Sov. Phys. - JEPT 41, 570 (1976).
39. A. Baratoff and L. Kramer, SQUID - Superconducting Quantum Interference Devices and Their Applications, H. D. Hahlbohm and H. Lübbig, Eds. (Walter de Gruyter, Berlin - New York, 1977).
40. J. Niemeyer and V. Kose, SQUID - Superconducting Quantum Interference Devices and Their Applications, H. D. Hahlbohm and H. Lübbig, Eds. (Walter de Gruyter, Berlin - New York, 1977).
41. D. G. McDonald, E. G. Johnson, and R. E. Harris, Phys. Rev. B13, 1028 (1976).
42. M. Tinkham, M. Octavio, and W. J. Skocpol, J. Appl. Phys. 48, 1311 (1977).

FIGURE CAPTIONS

Fig. 1. The equivalent circuit of (a) the junction, and (b) the rf and IF coupling, that were assumed in the simulations. The output circuit (c) of the junction was found to be valid for IF frequencies up to approximately 1/10 of the LO frequency.

Fig. 2. Examples of static I-V curves generated by a junction simulator for various values of normalized frequency, rf current, and noise parameter Γ . The dependence of the zero-voltage critical current on rf current shown at the bottom of the figure is reproduced from Ref. 15.

Fig. 3. The dependence of several S_N (defined in Eq. (7)) on normalized frequency.

Fig. 4. The dependence on normalized frequency of the parameters P, Q, and Γ_o , used in Eq. (22) to obtain the differential resistance.

Fig. 5. A comparison of the conversion efficiencies that would be expected for various orders N of harmonic mixing, for a range of normalized signal frequencies. It is assumed that the LO frequency is near ν_{sig}/N . The values chosen for r_s and Γ are plausible design goals; the results can be extended to different values of Γ using Eq. (8).

Fig. 6. (Dashed lines) Simulator predictions of noise parameter β^2 vs. bias voltage, for a junction with and without LO current applied.

Fig. 6. Also shown are the corresponding current-voltage curves (solid (cont.) lines). A subsequent recalibration revealed that the noise results shown are too high by $\sim 30\%$.

Fig. 7. The dependence of the noise parameters β_{\min}^2 , γ^2 , and β_{\min}^2/S_1^2 on normalized frequency, as deduced with the simulator.

Fig. 8. A typical sequence of I-V curves for a junction strongly coupled to the LO, using progressively larger values of driving noise Γ . The results are insensitive to the value of the (unloaded) Q of the rf coupling circuit.

Fig. 9. A demonstration of the effect on junction I-V curves of detuning the rf coupling circuit. The LO level has been adjusted in each case to yield the same suppression of the critical current.

Fig. 10. A summary of simulator results for the case of a strongly coupled junction. The mixer noise temperature and conversion efficiency are shown as functions of operating temperature, for the following junction parameters:

(A) $I_c = 110 \mu A$, R (ohms) = 0.1 ν (GHz)

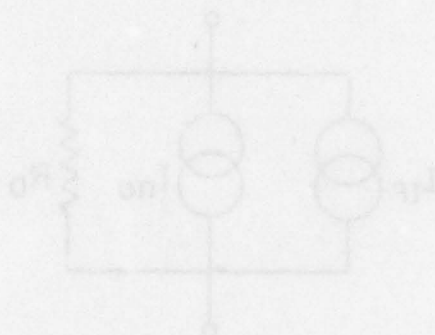
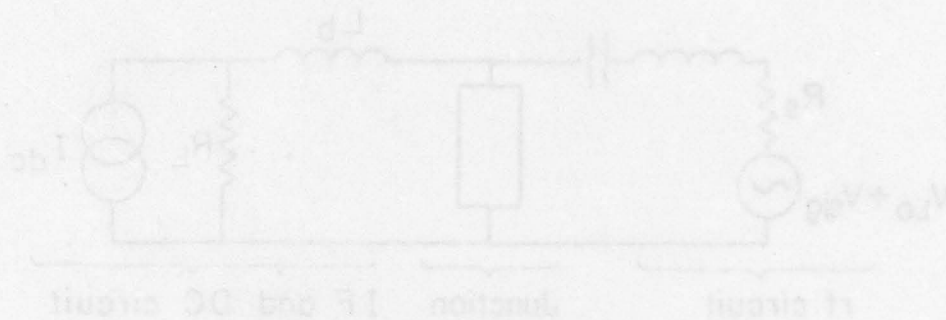
(B) $I_c = 11 \mu A$, R (ohms) = 1.0 ν (GHz)

(C) $I_c = 110 \mu A$, R (ohms) = 0.04 ν (GHz)

(D) $I_c = 11 \mu A$, R (ohms) = 0.4 ν (GHz)

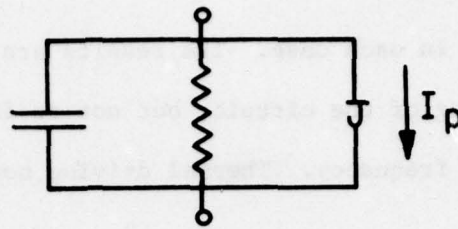
Note that (A) and (B) correspond to $\Omega = 0.19$, while (C) and (D) correspond to $\Omega = 0.47$. The unloaded Q of the coupling circuit

Fig. 10. was 20 in each case. The results are fairly sensitive to
(cont.) detuning of the circuit, but not to its Q when operated at its
center frequency. Thermal driving noise was assumed throughout.

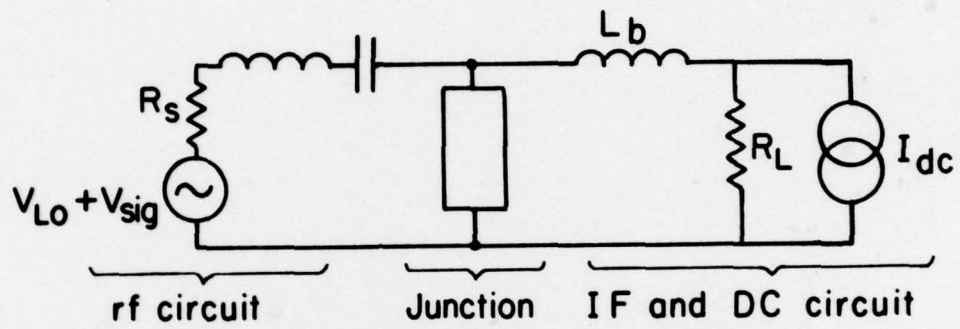


(c) Equivalent Low-Frequency Circuit

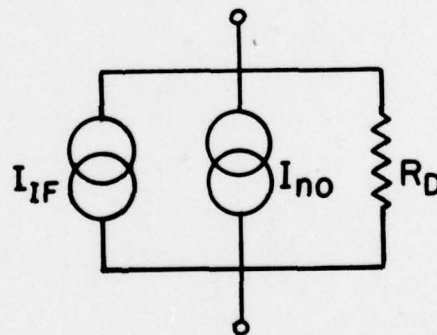
XSL 756-578W



(a) Junction Model



(b) External Coupling Model

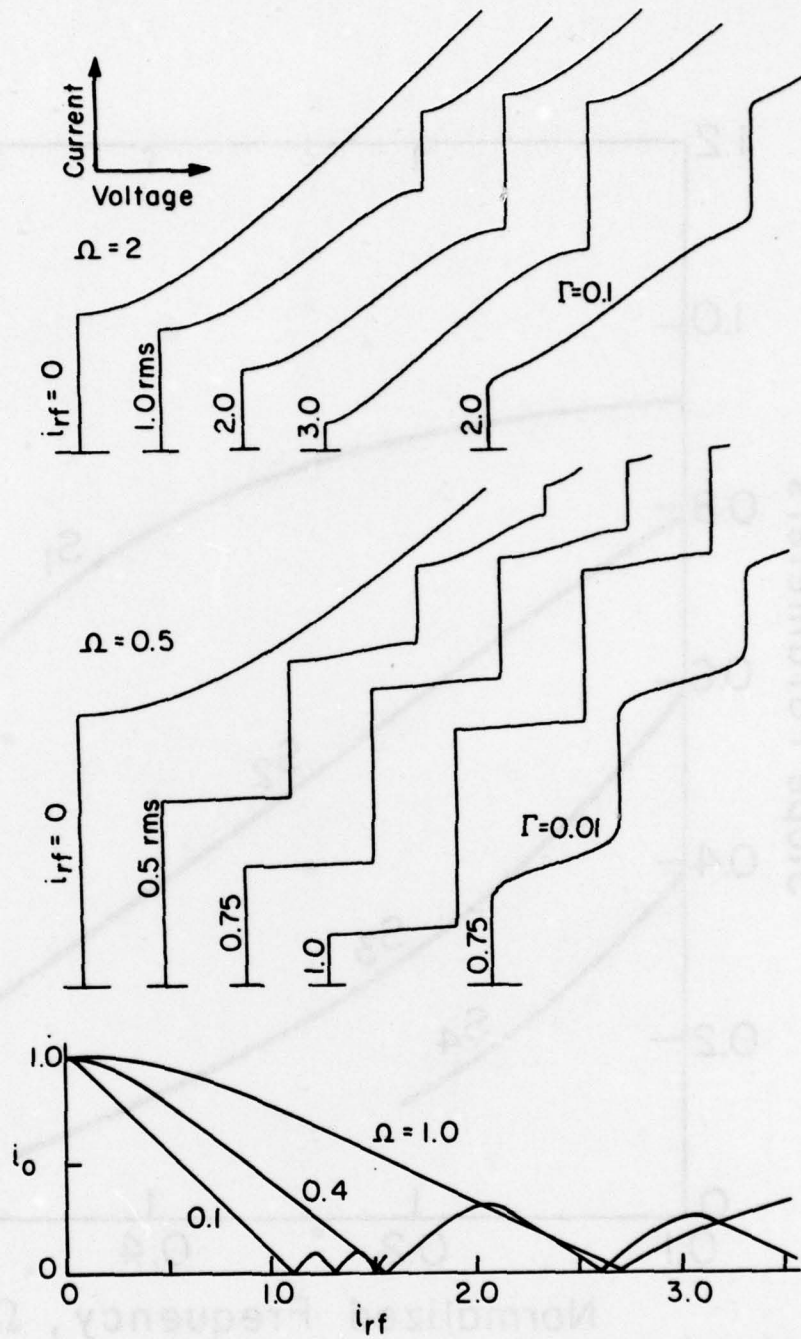


(c) Equivalent Low-Frequency Circuit

XBL 774-5384

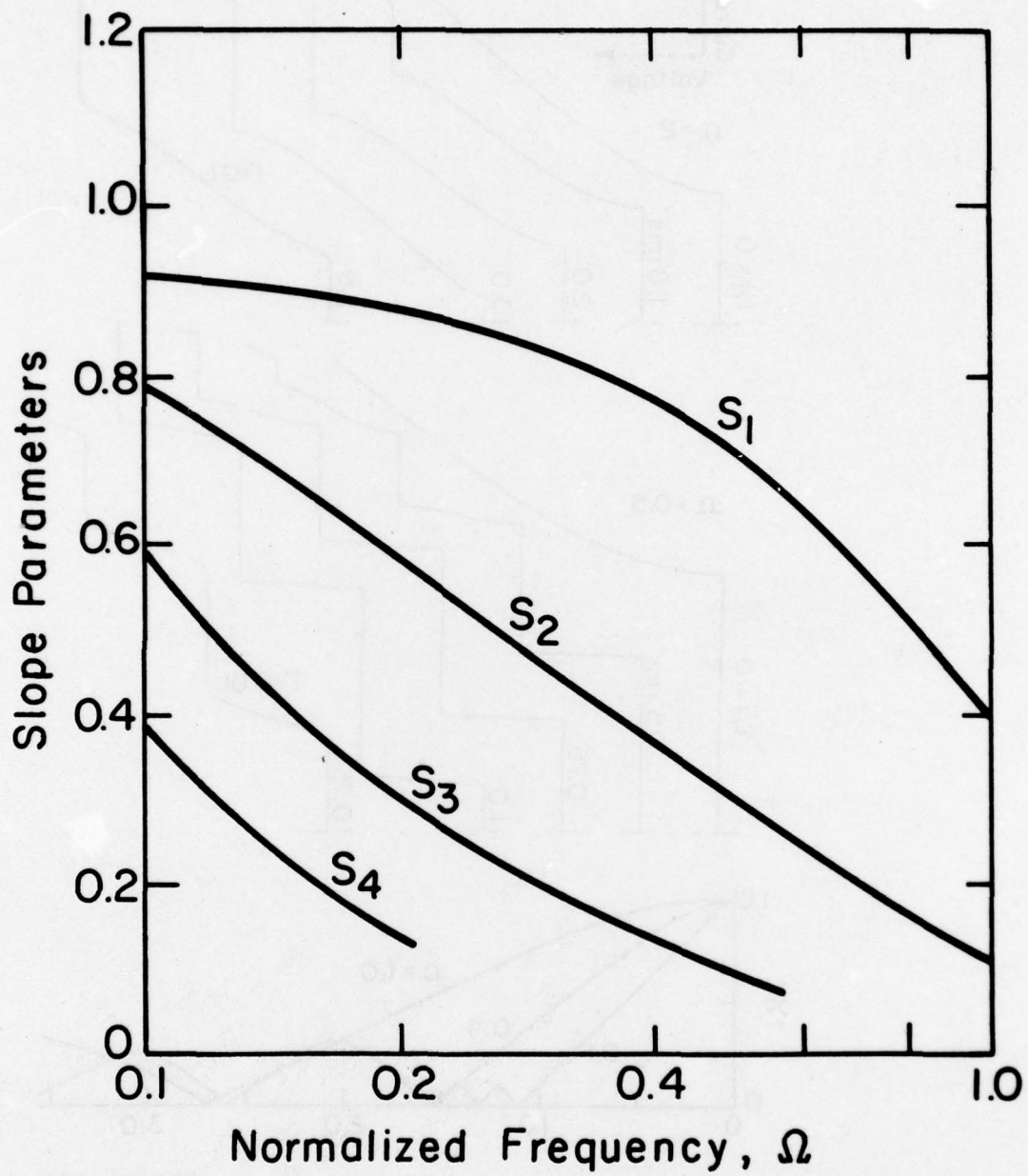
Fig. 1

Current Source Coupling



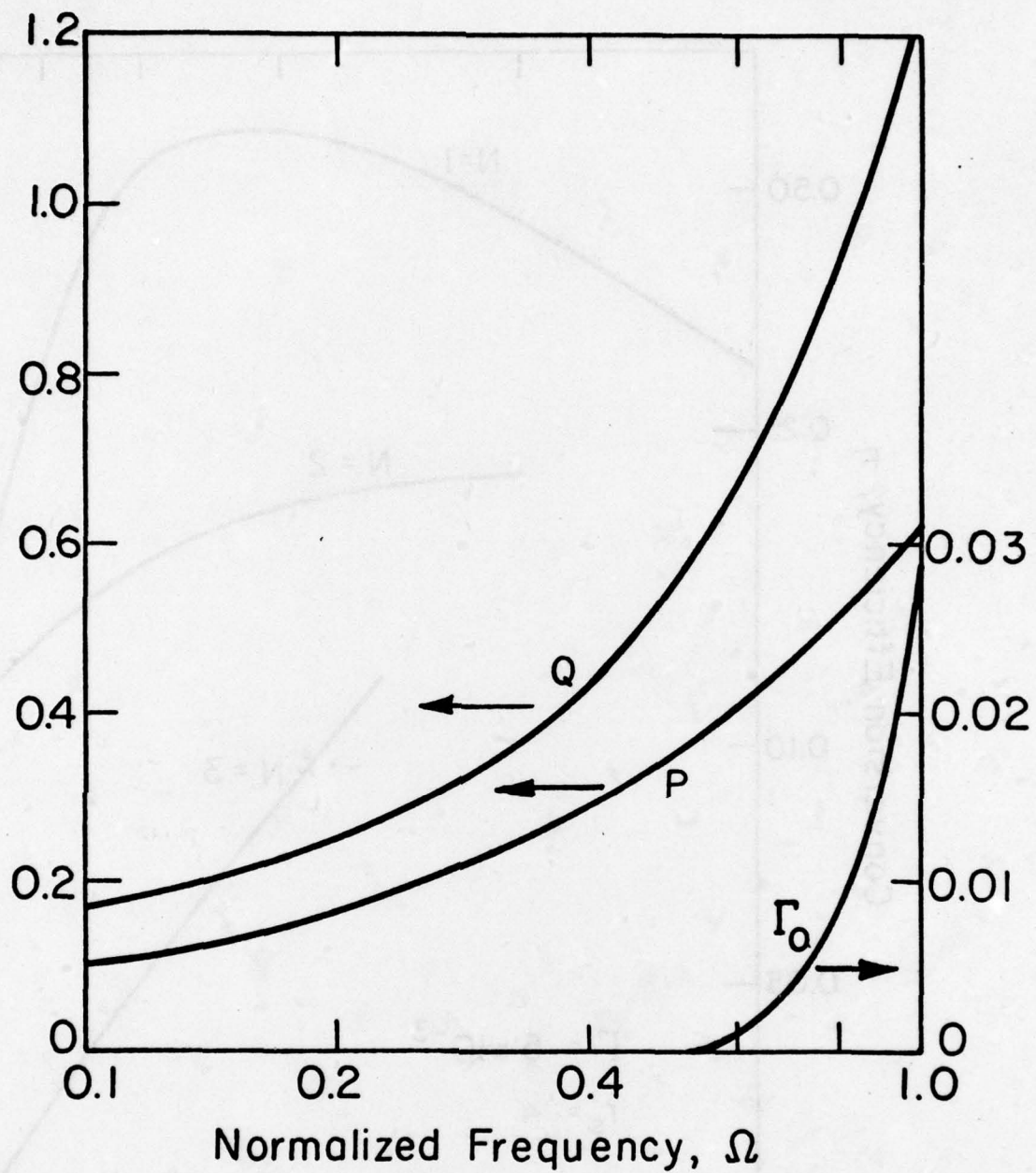
XBL 774-5381

Fig. 2



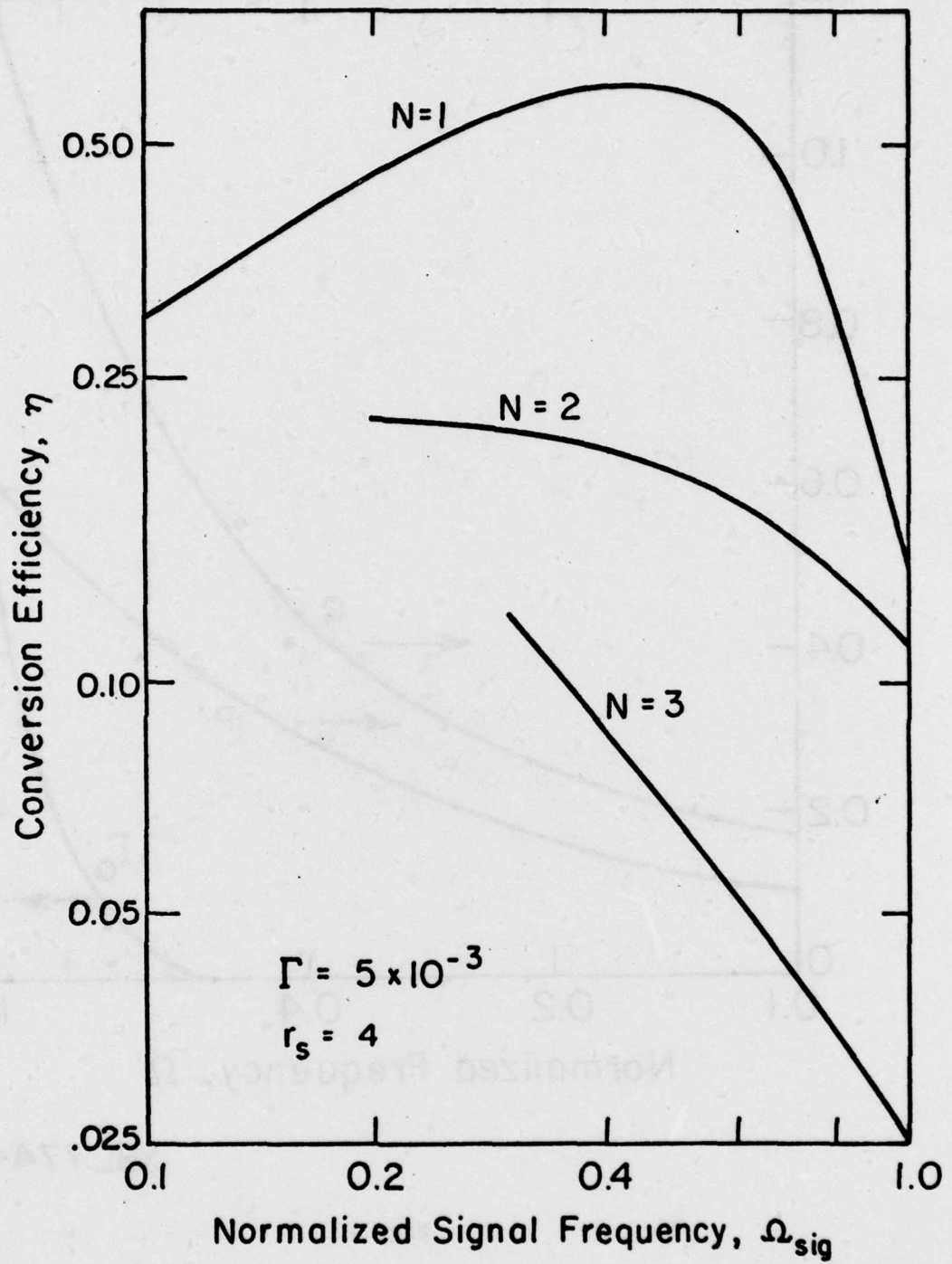
XBL 776-5639

Fig. 3



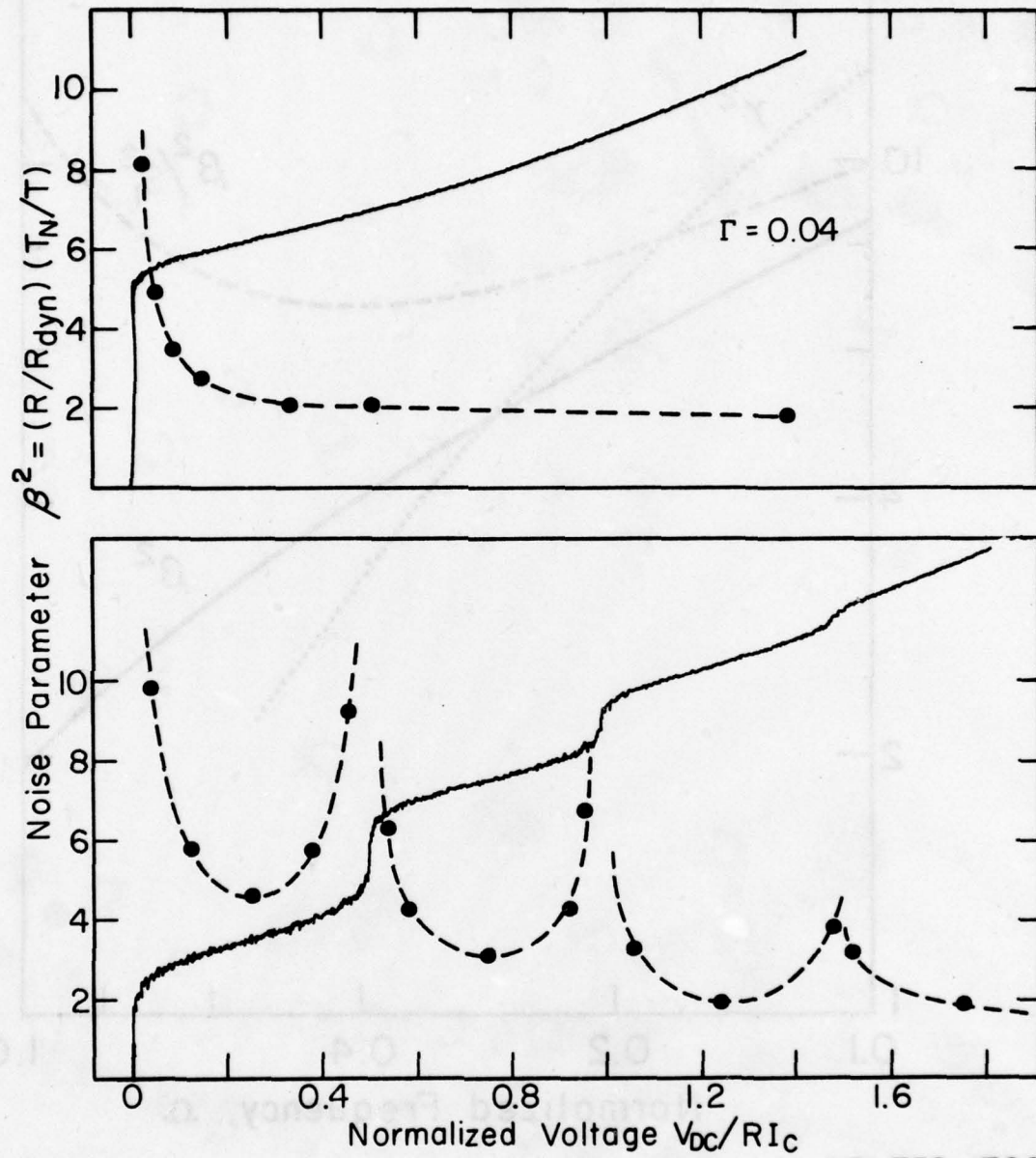
XBL 774-5392

Fig. 4



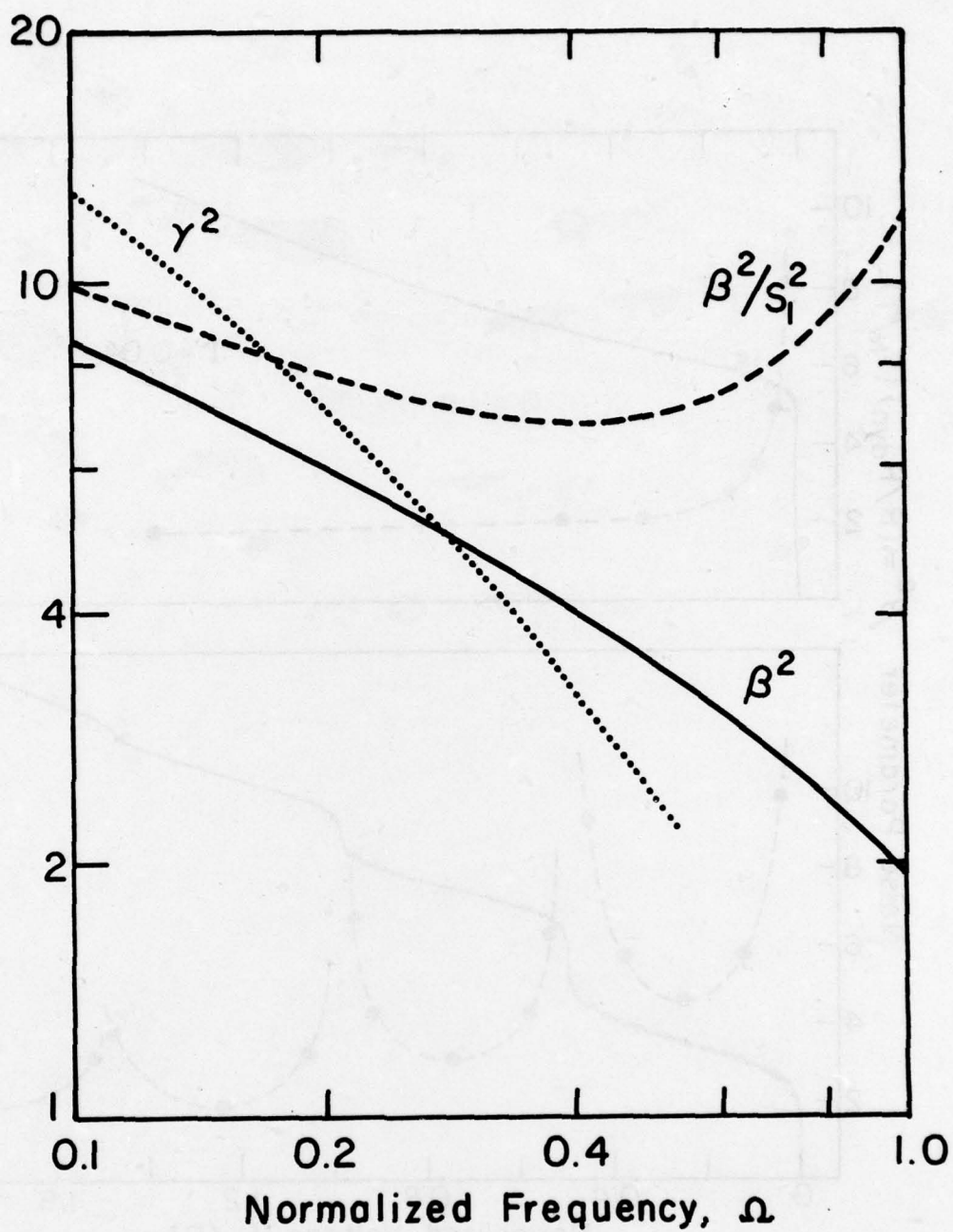
XBL774-5389

Fig. 5



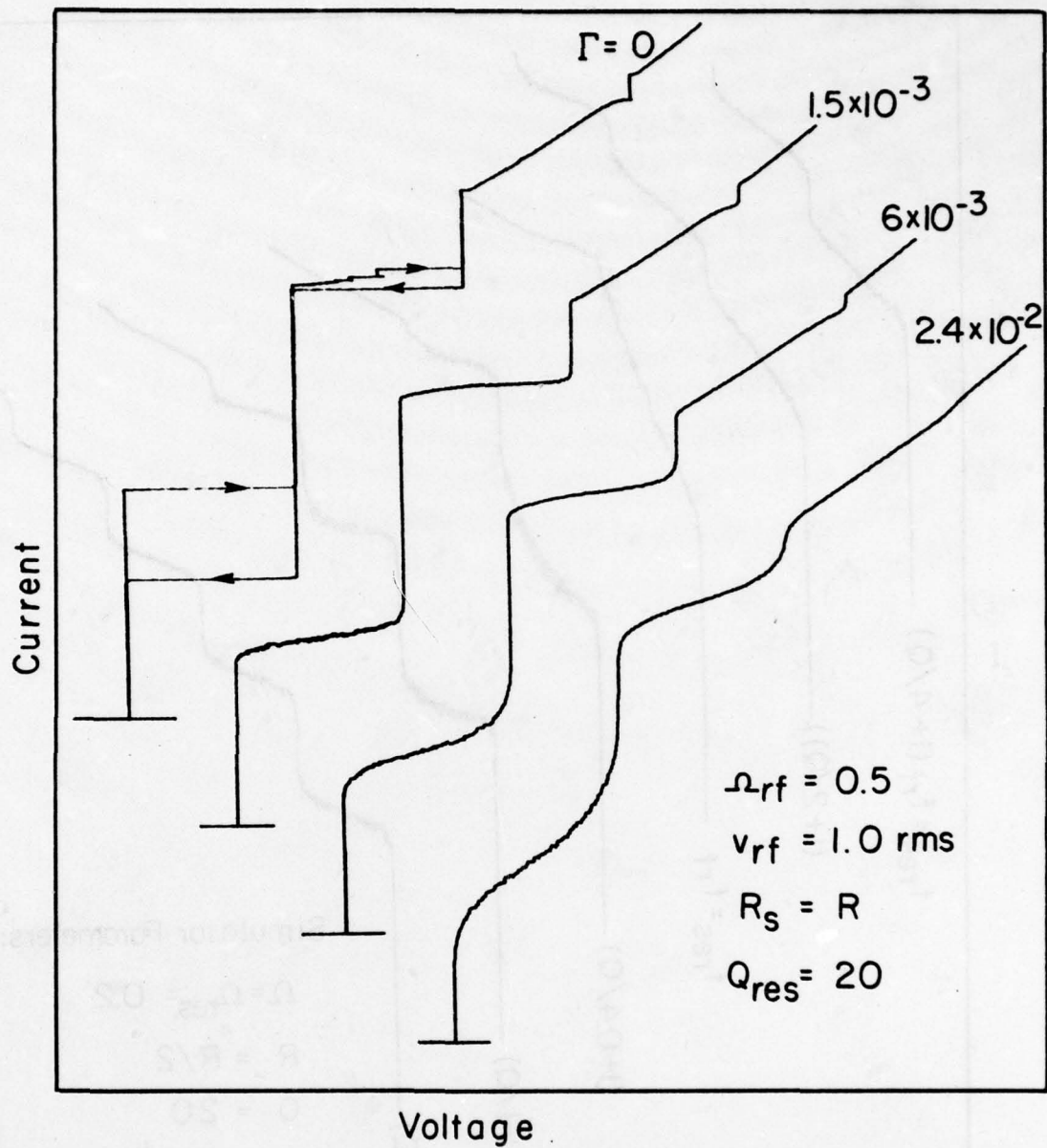
XBL738-1780A

Fig. 6



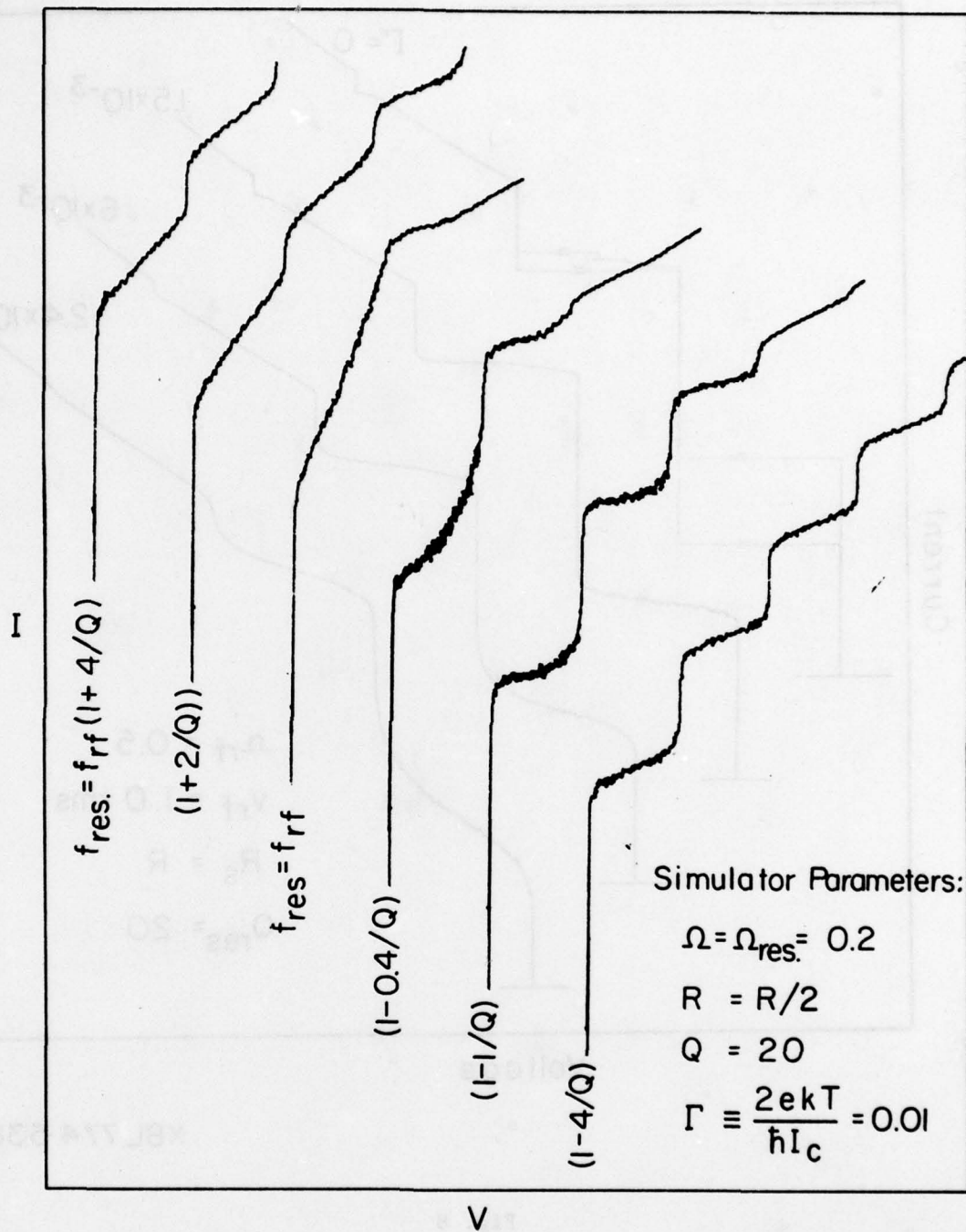
XBL 774-5390

Fig. 7



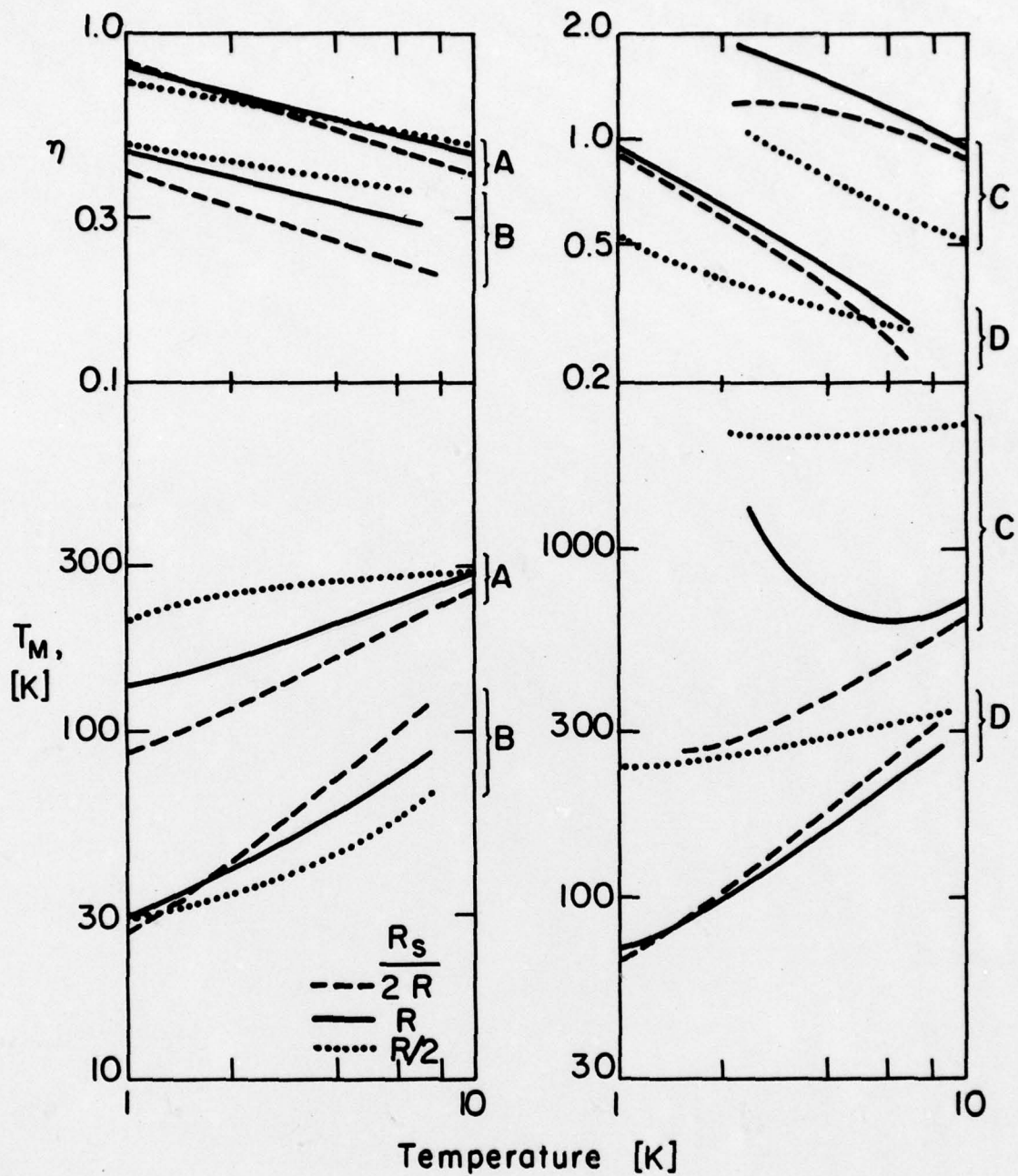
XBL 774-5380

Fig. 8



XBL 738-1749A

Fig. 9



XBL 774-539I

Fig. 10